Re-Face Stereospecificity of Methylene-tetrahydromethanopterin and Methylenetetrahydrofolate Dehydrogenases is Predetermined by Intrinsic Properties of the Substrate

Stefan Bartoschek,[a, b]+ Gerrit Buurman,[a]+ Rudolf K. Thauer,*[a] Bernhard H. Geierstanger,[b] Jan P. Weyrauch,[b] Christian Griesinger,*[b] Michael Nilges,[d] Michael C. Hutter,[c]+ and Volkhard Helms*[c]

Dedicated to Prof. Dr. Ernst-G. Jäger on the occasion of his 65th birthday

Four different dehydrogenases are known that catalyse the reversible dehydrogenation of N^5,N^{10}*-methylenetetrahydromethanopterin (methylene-*H_4*MPT) or* N^5,N^{10}*-methylenetetrahydrofolate (methylene-*H_4*F) to the respective* N^5,N^{10}*-methenyl compounds. Sequence comparison indicates that the four enzymes are phylogenetically unrelated. They all catalyse the* Re*-face-stereospecific removal of the* pro-R *hydrogen atom of the coenzyme's methylene group. The* Re*-face stereospecificity is in contrast to the finding that in solution the* pro-S *hydrogen atom of methylene-*H_4*MPT and of methylene-*H_4*F is more reactive to heterolytic cleavage. For a better understanding we determined the conformations of methylene-*H_4*MPT in solution and when enzyme-bound by using NMR spectroscopy and semiempirical quantum mechanical calculations. For the conformation free in solution we find an envelope conformation for the imidazolidine ring, with the flap at* N^{10}*. The methylene* pro-S *C–H bond is anticlinal and the methylene* pro-R *C–H bond is synclinal to the lone electron pair of* N^{10}*. Semiempirical quantum mechanical calculations of heats of formation of methylene-*H_4*MPT and methylene-*H_4*F indicate that changing this conformation into an activated one in which the* pro-S *C–H bond is antiperiplanar, resulting in the preformation of the leaving hydride, would require a* $\Delta\Delta H_f^\circ$ *of* $+53\ kJ\,mol^{-1}$ *for methylene-*H_4*MPT and of* $+51\ kJ\,mol^{-1}$ *for methylene-*H_4*F. This is almost twice the energy required to force the imidazolidine ring in the enzyme-bound conformation of methylene-*H_4*MPT* ($+29\ kJ\,mol^{-1}$) *or of methylene-*H_4*F* ($+35\ kJ\,mol^{-1}$) *into an activated conformation in which the* pro-R *hydrogen atom is antiperiplanar to the lone electron pair of* N^{10}*. The much lower energy for* pro-R *hydrogen activation thus probably predetermines the* Re*-face stereospecificity of the four dehydrogenases. Results are also presented explaining why the chemical reduction of methenyl-*H_4*MPT*$^+$ *and methenyl-*H_4*F*$^+$ *with* $NaBD_4$ *proceeds* Si*-face-specific, in contrast to the enzyme-catalysed reaction.*

KEYWORDS:

conformation analysis · dehydrogenases · enzyme catalysis · oxidoreductases · stereospecificity

Introduction

Tetrahydromethanopterin (H_4MPT)[**] and tetrahydrofolate (H_4F) are coenzymes of analogous structure (Figure 1). Both coenzymes are involved in the interconversion of C_1 units at the oxidation levels of formate (N^5-formyl; N^{10}-formyl; N^5,N^{10}-methenyl), formaldehyde (N^5,N^{10}-methylene) and methanol (N^5-methyl).[1, 2] H_4MPT is the C_1 carrier in methanogenic archaea and

[a] *Prof. Dr. R. K. Thauer, S. Bartoschek, Dr. G. Buurman*
Max-Planck-Institut für terrestrische Mikrobiologie
and
Laboratorium für Mikrobiologie des Fachbereichs Biologie der Philipps-Universität
Karl-von-Frisch-Strasse, 35043 Marburg (Germany)
Fax: (+49) 6421-178209
E-mail: thauer@mailer.uni-marburg.de

[b] *Prof. Dr. C. Griesinger, S. Bartoschek, Dr. B. H. Geierstanger, J. P. Weyrauch*
Institut für Organische Chemie der Universität Frankfurt
Marie-Curie-Strasse 11, 60439 Frankfurt a. M. (Germany)
and
Max-Planck-Institut für biophysikalische Chemie
Am Fassberg 11, 37077 Göttingen (Germany)
Fax: (+49) 69-79829128
E-mail: cigr@org.chemie.uni-frankfurt.de

[c] *Dr. V. Helms, Dr. M. C. Hutter*
Max-Planck-Institut für Biophysik
Kennedyallee 70, 60596 Frankfurt a. M. (Germany)
Fax: (+49) 69-6303251
E-mail: Volkhard.Helms@mpibp-frankfurt.mpg.de

[d] *Dr. M. Nilges*
Structural and Computational Biology Programme
EMBL Heidelberg
Meyerhofstrasse 1, 69117 Heidelberg (Germany)

[+] *These authors contributed equally to this work.*

[**] *For abbreviations see ref. [64].*

  1439-4227/01/02/07-08 $ 17.50+.50/0 CHEMBIOCHEM **2001**, 2, 530 – 541

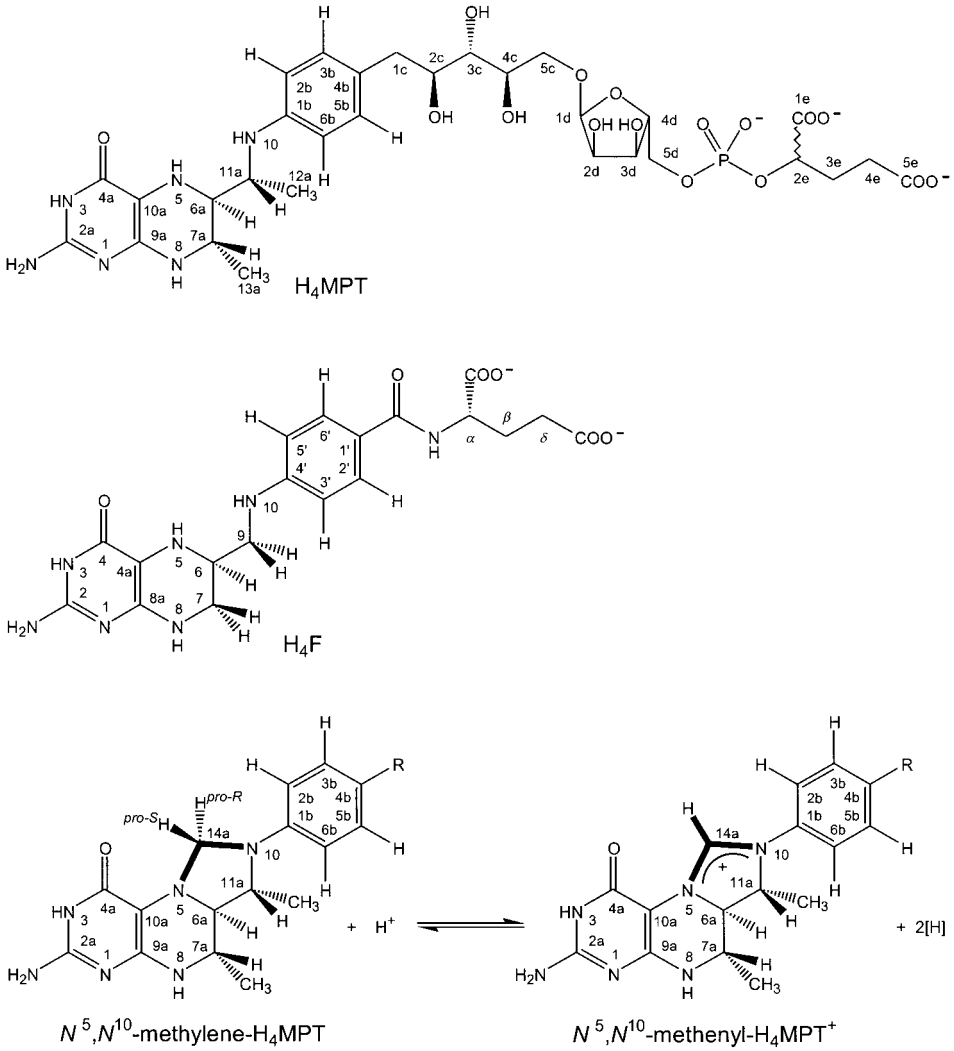

Figure 1. *Structures of tetrahydromethanopterin (H_4MPT), tetrahydrofolate (H_4F), N^5,N^{10}-methylene-H_4MPT and of N^5,N^{10}-methenyl-H_4MPT$^+$. The reversible dehydrogenation of the N^5,N^{10}-methylene compounds to the N^5,N^{10}-methenyl compounds is shown for methenyl-H_4MPT (bottom). The numbering scheme for H_4MPT was adopted from van Beelen et al.[61] and that for H_4F from Poe and Benkovic.[62] Functionally, the most important difference between H_4MPT and H_4F is the electron donating methylene group of H_4MPT in position 1 c, which is conjugated to N^{10} through the aromatic ring, whereas H_4F has an electron-withdrawing carbonyl group in this position. One consequence is that the redox potential of the N^5,N^{10}-methenyl-H_4MPT$^+$/N^5,N^{10}-methylene-H_4MPT couple (− 390 mV) is almost 100 mV more negative than that of the N^5,N^{10}-methenyl-H_4F$^+$/N^5,N^{10}-methylene-H_4F couple (− 300mV).[6]*

sulfate-reducing archaea, whereas H_4F serves this function in all other organisms. In methylotrophic bacteria both H_4MPT and H_4F are present.[3, 4] The interconversion of C_1 units is catalysed by specific cyclohydrolases (*N*-formyl ⇄ N^5,N^{10}-methenyl), dehydrogenases (N^5,N^{10}-methylene ⇄ N^5,N^{10}-methenyl + 2[H]) and reductases (N^5,N^{10}-methylene + 2[H] ⇄ N^5-methyl). Of these enzymes, the dehydrogenases catalyse the dehydrogenation of a prochiral center as shown for methylene-H_4MPT in Figure 1.

Four different families of methylenetetrahydromethanopterin and methylenetetrahydrofolate dehydrogenases are known:[5] 1) H_2-forming methylene-H_4MPT dehydrogenases (Hmd) found in many methanogenic archaea,[6, 7] 2) F_{420}-dependent methylene-H_4MPT dehydrogenases (Mtd) found in methanogenic archaea and sulfate-reducing archaea,[1] 3) NAD(P)-dependent methylene-H_4MPT dehydrogenases (MtdA and MtdB) found in methylotrophic bacteria[5, 8] and 4) NAD(P)-dependent methylene-H_4F dehydrogenases (e.g. FolD) found in all other organisms.[2, 9] These dehydrogenases catalyse the following reactions [Eqs. (1) – (4)]

$$\text{methylene-}H_4\text{MPT} + H^+ \xrightleftharpoons{\text{Hmd}} \text{methenyl-}H_4\text{MPT}^+ + H_2 \quad (1)$$
$$\Delta G^{0'} = +5.5\ \text{kJ mol}^{-1}$$

$$\text{methylene-}H_4\text{MPT} + H^+ + F_{420} \xrightleftharpoons{\text{Mtd}} \text{methenyl-}H_4\text{MPT}^+ + F_{420}H_2 \quad (2)$$
$$\Delta G^{0'} = -5.5\ \text{kJ mol}^{-1}$$

$$\text{methylene-}H_4\text{MPT} + \text{NAD(P)}^+ \xrightleftharpoons{\text{MtdA/B}} \text{methenyl-}H_4\text{MPT}^+ + \text{NAD(P)H} \quad (3)$$
$$\Delta G^{0'} = -13\ \text{kJ mol}^{-1}$$

$$\text{methylene-}H_4\text{F} + \text{NAD(P)}^+ \xrightleftharpoons{\text{FolD}} \text{methenyl-}H_4\text{F}^+ + \text{NAD(P)H} \quad (4)$$
$$\Delta G^{0'} = +3.5\ \text{kJ mol}^{-1}$$

As deduced from comparisons of the amino acid sequences, the four enzyme families are phylogenetically unrelated. However, within each of the four families all enzymes show sequence similarity even when they belong to organisms that are

phylogenetically very distantly related only. It thus appears that the four methylenetetrahydromethanopterin dehydrogenase families have evolved independently.[5] It is, therefore, surprising that the enzymatic dehydrogenation of methylene-H_4MPT and methylene-H_4F always leads to the removal of the *pro-R* hydrogen atom of the methylene group, that is, all four types of deydrogenases are *Re*-face-specific catalysts.[10–13]

Recently, for the H_2-forming methylenetetrahydromethanopterin dehydrogenase (Hmd) [Eq. (1)][14, 15] a mechanism of substrate activation was proposed that may be also valid for other methylenetetrahydromethanopterin and methylenetetrahydrofolate dehydrogenases. This mechanism is supported by ab initio molecular orbital calculations[16–18] and assumes that the methylene C—H bond of methylene-H_4MPT can only be cleaved heterolytically if it is activated in an antiperiplanar position to both lone electron pairs of the neighbouring N^5 and N^{10} atoms. In this position, the conjugation of the neighbouring n orbitals with the σ* orbital of the C—H fragment is maximal and thus the C—H bond is weakened, making it easier for the hydride ion to leave.[19–21]

In aqueous solution methylene-H_4MPT and methylene-H_4F are in a conformation in which the *pro-S* C—H bond is more reactive towards H^- formation than the *pro-R* C—H bond.[15] This was inferred from $^1J_{C,H}$ coupling constants and chemical shifts of the *pro-R* and *pro-S* protons and from the finding that the chemical reduction of methenyl-H_4MPT$^+$ and of methenyl-H_4F$^+$ in aqueous solution with $NaBD_4$ leads to the incorporation of the hydrogen into the *pro-S* position of the methylene group.[15] In aqueous solution the imidazolidine ring of methylene-H_4MPT was therefore assumed to be in an envelope conformation with C^{14a} above the ring and the *pro-S* proton at C^{14a} in antiperiplanar position to the lone electron pairs of N^5 and N^{10} (Figure 2 A).[15] The *pro-R* hydrogen atom at C^{14a} would be in a position synclinal to the lone electron pairs of the two neighbouring nitrogen atoms and thus should not be activated.

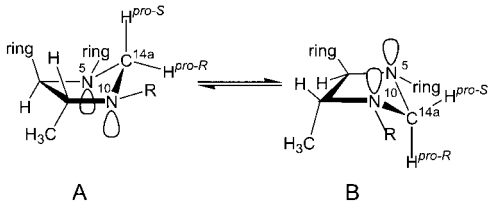

Figure 2. *Previously proposed conformations of the imidazolidine ring of methylene-H_4MPT: A) free in solution and B) bound to H_2-forming methylene-H_4MPT dehydrogenase (Hmd). In both cases, the imidazolidine ring is in an envelope conformation with the flap C^{14a} A) above or B) below the ring.[15] From the heats of formation (ΔH_f°), the energy change ΔE_{AB} associated with a conformational change between the two conformers was calculated to be larger than + 200 kJ mol^{-1} (see Results section).*

Editorial Advisory Board Member:[*]
Rudolf K. Thauer,

born in Frankfurt (Germany) in 1939, studied biochemistry at the universities of Frankfurt, Tübingen and Freiburg, where he obtained his PhD degree in the laboratory of Karl Decker in 1968. After his habilitation in Freiburg and a three-months stay in Harland Wood's laboratory in Cleveland (Ohio) he was appointed Associate Professor of Biochemistry at the University of Bochum in 1972. Since 1976 he is Professor of Microbiology at the Philipps University Marburg, and since 1991 he is also Director at the Max Planck Institute for Terrestrial Microbiology in Marburg. His studies are focused on the C_1 metabolism of methanogenic archaea. His group was involved in unravelling the structure and function of many of the novel enzymes and coenzymes involved in CO_2 reduction to methane, a recent example being the crystal structure of nickel-containing methyl-coenzyme M reductase which catalyses the methane-forming reaction proper. Another interesting discovery was that methanogens contain an enzyme that catalyses a reaction with H_2 as substrate without the apparent involvement of a redox-active transition metal. This "metal-free" hydrogenase (Hmd) is also subject of the investigation reported here.

[*] *Members of the Editorial Advisory Board will be introduced to the readers with their first manuscript.*

Since the *pro-R* C—H bond rather than the *pro-S* C—H bond is cleaved in the enzyme-catalysed dehydrogenation of methylene-H_4MPT, it was proposed that upon binding to the enzyme methylene-H_4MPT must be forced into a conformation in which the *pro-R* hydrogen atom is reactive or easily activated.[14, 15] Figure 2 B shows the proposed conformation for the enzyme-bound methylene-H_4MPT in the transition state. With C^{14a} below the ring, the *pro-S* hydrogen atom is in a synclinal position to the lone electron pairs, and the *pro-R* proton is in an antiperiplanar position to the lone electron pairs of N^5 and N^{10}. The *pro-R* C—H bond in conformation B should therefore be maximally reactive.

Whether binding to dehydrogenases induces such a conformational change in the coenzyme remains speculative since currently no structures of methylene-H_4MPT or of methylene-H_4F alone or in complex with any dehydrogenase are available. The structure of methenyl-H_4F$^+$ has been solved by X-ray crystallography.[22] This structure agrees well with NMR spectroscopic studies on the conformations of the tetrahydropyrazine and imidazolidine rings of methylene-H_4F.[23, 24] However, the exact conformation of the imidazolidine ring at N^{10} in methylene-H_4F was not clearly defined and was suggested to be sp^3-hybridised in the structure reported by Poe and Benkovic[23] and to be sp^2-hybridised in that reported by Kalbermatten et al.[24]

Here we use two-dimensional nuclear Overhauser effect spectroscopy (NOESY) to study the conformation of methylene-H_4MPT in solution and when bound to H_2-forming methylene-H_4MPT dehydrogenase (Hmd) from methanogenic archaea. Because the enzyme-bound and the free forms of methylene-H_4MPT are exchanging rapidly on the NMR time scale, we were able to utilise the concept of transferred NOE spectroscopy

(Tr-NOESY)[25–27] to characterise the conformation of methylene-H_4MPT when bound to the enzyme. We show that both conformations are in an envelope conformation with the flap N^{10} below (free in solution) or above (bound to enzyme) the imidazolidine ring. The conformational change between the free and the enzyme-bound forms is smaller than proposed previously (Figure 2).[15] For the transition state of the methylene-H_4MPT oxidation, a conformation with a reactive *pro-R* C–H bond is proposed which, according to semiempirical quantum mechanical calculations, is significantly lower in energy than that of the conformation with a reactive *pro-S* C–H bond. In contrast to the previously proposed reactive conformation, the *pro-R* C–H bond is antiperiplanar to the lone electron pair of only one nitrogen atom. In addition, we describe results from theoretical calculations that explain the reversed stereospecificity of the enzyme-catalysed relative to the uncatalysed chemical reduction of methenyl-H_4MPT^+ and methenyl-H_4F^+.

Results

Conformation of methylene-H_4MPT in aqueous solution and when bound to Hmd as determined by NMR spectroscopy

Two-dimensional NOESY was used to study the conformation of methylene-H_4MPT in aqueous solution (Figure 3) and when bound to H_2-forming methylene-H_4MPT dehydrogenase (Hmd) from *Methanothermobacter marburgensis* (formerly *Methanobacterium thermoautotrophicum*).[28] The spectra of methylene-H_4MPT were acquired under strictly anaerobic conditions at 0 °C and pH 7.8. Under these conditions methylene-H_4MPT and the enzyme Hmd are relatively stable and the equilibrium of the reaction of methylene-H_4MPT to methenyl-H_4MPT^+ [Eq. (1)] is far to the side of methylene-H_4MPT.

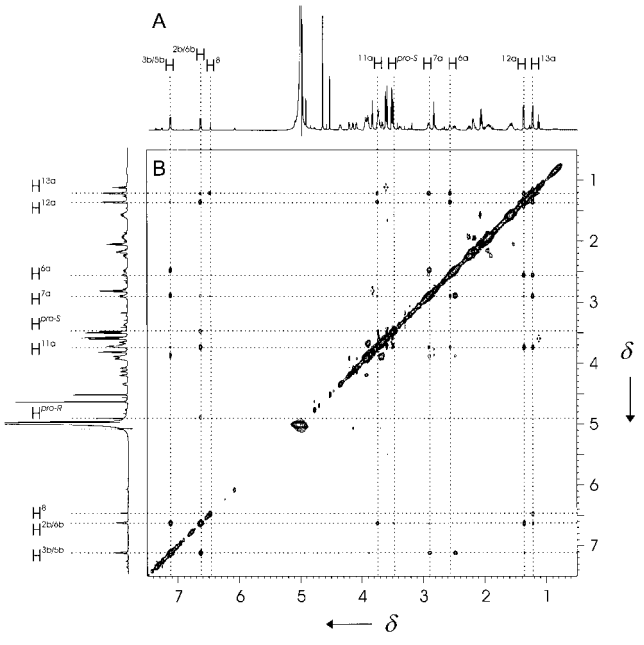

Figure 3. *A) One-dimensional ^{1}H NMR spectrum of 1 mM methylene-H_4MPT in H_2O/D_2O (9:1) containing 50 mM K_2HPO_4/KH_2PO_4 (pH 7.8) at 0 °C. B) Two-dimensional NOESY spectrum of the same sample obtained with a mixing time of 50 ms. The NMR spectra were acquired at a ^{1}H frequency of 600.13 MHz on a DRX 600 spectrometer (Bruker Instruments, Rheinstetten) and processed as described in the Experimental Section.*

The signals of all individual protons and of magnetically equivalent proton pairs of methylene-H_4MPT were assigned according to published spectra.[11] To determine the conformation at N^{10}, through-space NOE contacts of the proton pair $H^{2b/6b}$ of the aromatic ring with the protons H^{6a}, H^{7a}, H^{12a}, H^{11a}, $H^{pro\text{-}R}$, $H^{pro\text{-}S}$ and H^{13a} (see Figure 1) are most important. Figure 4 shows the traces through the NOESY spectrum along the signal of the aromatic $H^{2b/6b}$ protons of methylene-H_4MPT in the absence (Figure 4 A) and in the presence of Hmd (Figure 4 B). Distances between protons (Table 1) were obtained from NOE build-up curves (Figures 5 A and B) and used in a restrained simulated annealing and energy minimisation protocol as described in detail in the Experimental Section. For the free form as well as for the enzyme-bound form the rotation of the two methyl groups and of the aromatic ring had to be taken into account, because of 40 model structures derived from two starting geometries, none fully satisfied the NMR distance restraints. Ensembles of structures were therefore generated by stepwise rotating the aromatic ring and the methyl groups and by calculating the effects of NOE averaging [Eqs. (7) – (9) in the Experimental Section].

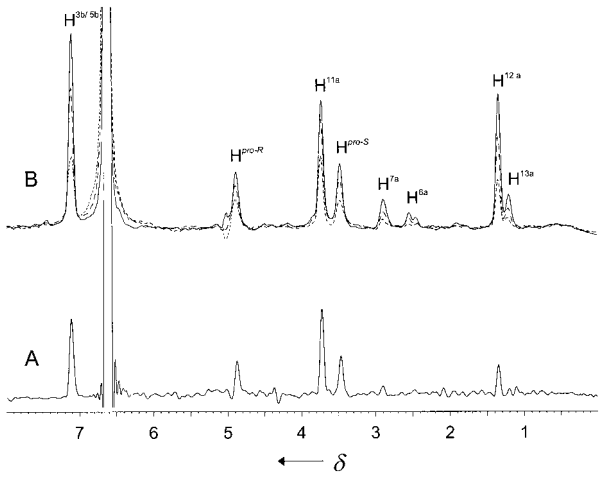

Figure 4. *Traces through a two-dimensional NOESY spectrum of methylene-H_4MPT along the signal of the $H^{2b/6b}$ protons of the aromatic ring (see Figure 3 B). A) Methylene-H_4MPT in the absence and B) methylene-H_4MPT in the presence of H_2-forming methylene-H_4MPT dehydrogenase (Hmd) both in anaerobic solution at 0 °C. The concentration of methylene-H_4MPT was 1.0 mM and that of Hmd 0.3 mM (ca. 6 mg protein in 0.5 mL). After the acquisition of four NOESY spectra over a period of 48 h the Hmd activity had decreased by 50 %. In the presence of enzyme the peak volumes increased by a factor of four. A) ——, 50 ms mixing time; B) ——, 50 ms mixing time; – – –, 30 ms mixing time; - - - -, 15 ms mixing time.*

In the resulting conformation of methylene-H_4MPT free in solution (Figure 6, conformation **Ia**) the imidazolidine ring is in an envelope conformation with the flap at N^{10}, and the methylene *pro-S* C–H bond is anticlinal and the methylene *pro-R* C–H bond is synclinal to the lone electron pair of N^{10}.

The conformation of methylene-H_4MPT when bound to Hmd could be determined in a similar manner. The trace through the

Table 1. *Intramolecular distances between protons of methylene-H_4MPT free in solution and when bound to H_2-forming methylene-H_4MPT dehydrogenase (Hmd).*[a]

Proton pair			Methylene-H_4MPT free in solution		Methylene-H_4MPT in the presence of Hmd	Methylene-H_4MPT bound to Hmd	
A	B	$\frac{\sigma^{a}_{A-B}}{\sigma^{a}_{ref}}$[b]	$r_{A\text{-}B(free)}$ [Å][c]	$\bar{r}_{A\text{-}B(free)}$ [Å][d]	$\frac{\sigma^{p}_{A-B}}{\sigma^{p}_{ref}}$[b]	$r_{A\text{-}B(bound)}$ [Å][c]	$\bar{r}_{A\text{-}B(bound)}$ [Å][d]
$H^{2b/6b}$	$H^{3b/5b}$	1.0000	2.46	2.46	1.0000	2.46	2.46
$H^{2b/6b}$	H^{12a}	0.1074	3.57	4.36	0.3369	2.91	2.61
$H^{2b/6b}$	H^{7a}	0.1633	3.33	3.25	0.0279	5.27	5.28
$H^{2b/6b}$	$H^{pro\text{-}S}$	0.4150	2.85	2.62	0.4269	2.83	2.81
$H^{2b/6b}$	H^{11a}	0.8598	2.52	2.42	0.5296	2.77	3.20
$H^{2b/6b}$	$H^{pro\text{-}R}$	0.2665	3.07	3.25	0.3239	2.96	2.62
H^{6a}	$H^{2b/6b}$	0.0097	5.33	5.12	0.0273	4.42	4.62
$H^{2b/6b}$	H^{13a}	0.0394	4.22	5.57	0.0077	6.29	6.51
H^{11a}	H^{13a}	0.4881	2.77	2.65	0.3272	3.00	2.72
H^{7a}	H^{13a}	0.4070	2.86	2.60	0.5074	2.74	2.42
H^{6a}	H^{13a}	0.2912	3.02	2.75	0.2667	3.07	3.09
H^{11a}	H^{12a}	0.4249	2.84	2.60	0.3880	2.89	2.59
H^{7a}	H^{12a}	0.0140	5.01	4.59	0.0472	4.03	4.06
H^{6a}	H^{12a}	0.5134	2.75	2.51	0.3213	3.01	2.51
H^{11a}	H^{6a}	0.4197	2.84	2.91	0.2368	3.18	3.09
H^{11a}	H^{7a}	0.7297	2.59	2.45	1.1851	2.37	2.20
H^{6a}	H^{7a}	0.2683	3.06	3.13	0.6266	2.63	3.11
H^{7a}	$H^{pro\text{-}S}$	0.2647	3.07	3.21	0.2568	3.09	4.01
H^{12a}	$H^{pro\text{-}S}$	0.0181	4.80	4.11	0.0303	4.37	4.49
$H^{pro\text{-}S}$	$H^{pro\text{-}R}$	2.7750	2.08	1.84	0.6560	2.89	1.83
H^{12a}	$H^{pro\text{-}R}$	0.0404	4.20	3.82	0.0420	4.17	4.20
H^{8}	H^{13a}	0.3763	2.90	2.79	0.1465	3.52	3.62
H^{8}	H^{7a}	0.6530	2.64	2.54	0.2252	3.31	2.54
H^{11a}	$H^{pro\text{-}S}$	0.1156	3.52	3.73	0.0407	4.39	3.57

[a] Distances r were calculated from NOE cross-relaxation rates that were determined from the initial slopes of the NOE build-up curves acquired at 0 °C (Figure 5) as described in the Experimental Section. The proton pairs containing the aromatic protons $H^{2b/6b}$ are listed first. [b] $\sigma_{A\text{-}B}$ is the cross-relaxation rate between protons A and B; $\sigma_{H^{2b/6b}\text{-}H^{3b/5b}}$ the cross-relaxation rate of the proton pairs $H^{2b/6b}$ and $H^{3b/5b}$, which have a fixed distance of 2.46 Å, served as reference rate σ_{ref}. The reference cross-relaxation rate in the absence of enzyme is referred to as σ^{a}_{ref} and in the presence of enzyme as σ^{p}_{ref}. [c] The distance between protons A and B, $r_{A\text{-}B}$, is determined according to: $(r_{A\text{-}B} = r_{H^{2b/6b}\text{-}H^{3b/5b}}(\sigma_{ref}/\sigma_{A\text{-}B})^{1/6})$. For methylene-$H_4$MPT bound to Hmd, the contributions of the free conformation to the observed NOE cross-relaxation rates were subtracted as described in the Experimental Section. [d] $\bar{r}_{A\text{-}B(free)}$ are the average distances in conformation **Ia** and $\bar{r}_{A\text{-}B(bound)}$ are the average distances in conformation **IIa** (Figure 6) taking the rotation of the two methyl groups and of the aromatic ring into account (see Experimental Section).

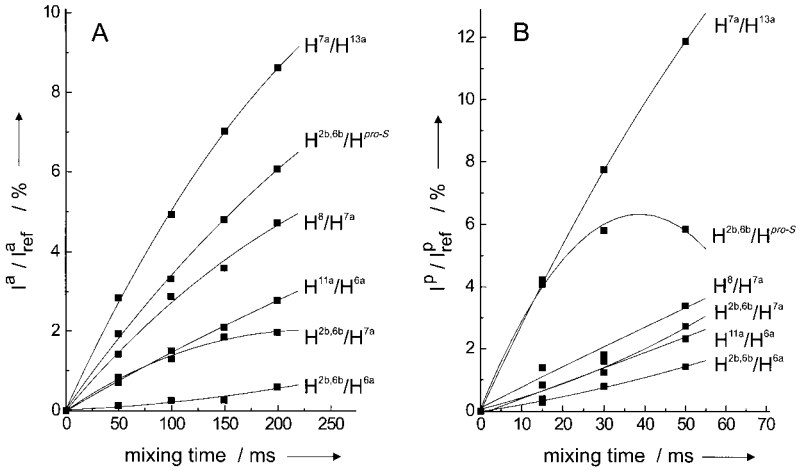

Figure 5. *NOE build-up curves for several proton pairs in methylene-H_4MPT at 0 °C A) in the absence (index a) and B) in the presence (index p) of H_2-forming methylene-H_4MPT dehydrogenase (Hmd) in arbitrary units as determined from cross-peak integrals at different mixing times (see Figure 4).*

two-dimensional NOESY spectrum along the signal of the aromatic $H^{2b/6b}$ protons of methylene-H_4MPT in the presence of Hmd shows only one set of coenzyme resonances (Figure 4 B). This indicates that the enzyme-bound and the free forms of methylene-H_4MPT are in a fast exchange on the NMR time scale. The observed NOE cross-peaks are therefore the sum of contributions from NOE interactions in free and enzyme-bound methylene-H_4MPT. For the same NOESY mixing time (50 ms) the NOE integral of the $H^{2b,6b}/H^{3b,5b}$ protons, which have a fixed distance of 2.46 Å (calibration NOE), is fourfold larger in the presence of enzyme (Figure 4 B) than for free methylene-H_4MPT (Figure 4 A). Because the NOE increases with molecular mass, an intensity increase of intramolecular NOE (as shown in Figure 4) is a clear indication of methylene-H_4MPT binding to Hmd under the conditions of the experiment. The increase in the calibration NOE by a factor of 4 in the presence of enzyme indicates that all NOE intensities in the presence of enzyme will be dominated by contributions from the bound form of methylene-H_4MPT, a prerequisite for transferred NOE studies.[26, 27] In addition, some proton – proton distances in the bound form change relative to those in the free form, as can be judged from the slope of the build-up curves (Figure 5).

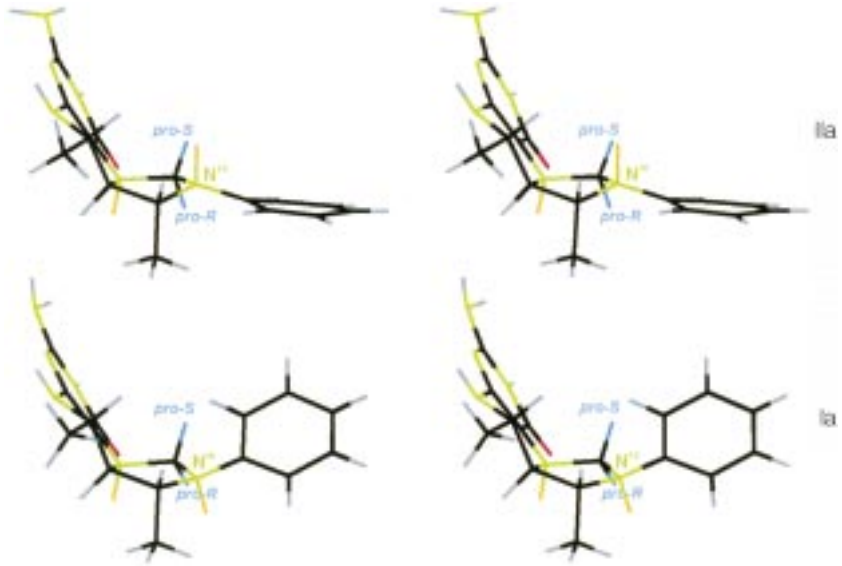

Figure 6. *Conformations (stereoview) of the imidazolidine ring of methylene-H_4MPT free in solution (**Ia**) and bound to H_2-forming methylene-H_4MPT dehydrogenase (Hmd) (**IIa**) as determined by NMR spectroscopy. The conformations were calculated using a restrained simulated annealing and energy minimisation protocol (see Experimental Section). Lone electron pairs are shown in yellow, hydrogens in blue, nitrogens in green, carbons in black and oxygens in red. The conformation of the aromatic ring was assumed to populate all dihedral angles between N^{10} and C^{16}.*

As in the case of the free form of methylene-H_4MPT, we used NOE build-up rates, simulated annealing and restrained energy minimisation to obtain the conformation of methylene-H_4MPT when bound to Hmd (Figure 6, conformation **IIa**). The imidazolidine ring is again in an envelope conformation with the flap at N^{10}, but in contrast to the free form the lone electron pair of N^{10} is anticlinal to the *pro-R* C—H bond and synclinal to the *pro-S* C—H bond. This conformational change is mainly represented by the change of interproton distances between $H^{2b/6b}$ and H^{6a}, between $H^{2b/6b}$ and H^{7a}, and between $H^{2b/6b}$ and H^{12a} (see Figures 1 and 6): From methylene-H_4MPT free in solution to methylene-H_4MPT bound to the enzyme the distance $r_{A\text{-}B}$ between $H^{2b/6b}$ and H^{6a} changes by 21%, between $H^{2b/6b}$ and H^{7a} by 37% and between $H^{2b/6b}$ and H^{12a} by 23%, respectively (see Table 1).

From the NOE cross-correlation rate of the proton pair $H^{2b/6b}$/$H^{3b/5b}$ of methylene-H_4MPT free in solution ($\sigma^{a}_{ref} = 0.2$ Hz) and in the presence of enzyme ($\sigma^{p}_{ref} = 1.5$ Hz) and from the molecular masses of methylene-H_4MPT and Hmd, the percentage of methylene-H_4MPT bound to the enzyme was calculated to be 14% as described in the Experimental Section [Eq. (5)]. It has to be considered, however, that the protein preparation contained an unknown amount of inactive protein formed by denaturation under the analysis conditions. Therefore, we refrain from calculating K_d from the measurements.

Energy-minimised conformations of the imidazolidine ring of methylene-H_4MPT and activation barriers calculated from heats of formation

Semiempirical AM1 calculations[29] were used to compute local energy minima for the conformations of methylene-H_4MPT. In the following, relative energies of two different conformations **A** and **B** will be labelled as ΔE_{AB} denoting the difference of the corresponding heats of formation ΔH°_{f} that were computed by AM1 for the conformations **A** and **B**. Two low-energy conformations were found (conformations **Ib** and **IIb** in Figure 7), differing only by 2 kJ mol^{-1}, which may be within the precision of the method. Particularly the conformation of the imidazolidine ring is in excellent agreement with the results of an ab initio optimisation (restricted Hartree–Fock/3-21G) of methylene-H_4MPT truncated after the phenyl ring.[65] Ignoring the relative orientations of the freely rotating aromatic ring, the two conformations are very similar to the conformations of methylene-H_4MPT determined by NMR spectroscopy (Figure 6). Conformation **Ib** in Figure 7 corresponds to conformation **Ia** in Figure 6 (methylene-H_4MPT free in solution), and conformation **IIb** in Figure 7 corresponds to conformation **IIa** in Figure 6 (methylene-H_4MPT bound to Hmd). The root-mean square (rms) deviations between calculated and experimental structures are 0.23 Å and 0.21 Å (superimposing all heavy atoms in the three fused rings and C^{1b} of the freely rotating phenyl ring), respectively. The good agreement with more accurate ab initio quantum mechanical methods and with experimental NMR data lends confidence in applying semiempirical quantum mechanical methods to these systems.

Using semiempirical quantum mechanical calculations we calculated heats of formation for the different conformations of methylene-H_4MPT shown in Figure 7 and also for the initially proposed transition state (Figure 2B). The heats of formation for the putative enzyme-bound conformation **IIb** (Figure 7) and the initially proposed transition state (Figure 2B) differ by more than +200 kJ mol^{-1}. Such a high activation energy barrier between enzyme-bound substrate in the ground state and in the transition state and an experimentally determined activation barrier of approximately 50 kJ mol^{-1} for the enzymes from *M. marburgensis*[66] and from *Methanopyrus kandleri*[30] make it very unlikely that the reactive *pro-R* C—H bond is antiperiplanar to both lone electron pairs of N^5 and N^{10}.

For the different methylene-H_4MPT conformations shown in Figure 7 the heats of formation are displayed in Figure 8 as a function of the dihedral angle between the lone electron pair of N^{10} and the C^{14a}—$H^{pro\text{-}S}$ bond (Figure 8A) or the C^{14a}—$H^{pro\text{-}R}$ bond (Figure 8B). In the enzyme-bound conformation **IIb** (Figure 7) the methylene *pro-R* C—H bond has a dihedral angle of 143° with the lone electron pair of N^{10} (Table 2). For maximum reactivity of the *pro-R* C—H bond, the dihedral angle would have to be 180° as in conformation **III** (Figure 7), which is proposed to be the conformation in the transition state. Figure 8B shows that a ΔE_{23} of +29 kJ mol^{-1} is required for the conversion of conformation **IIb** into conformation **III**.

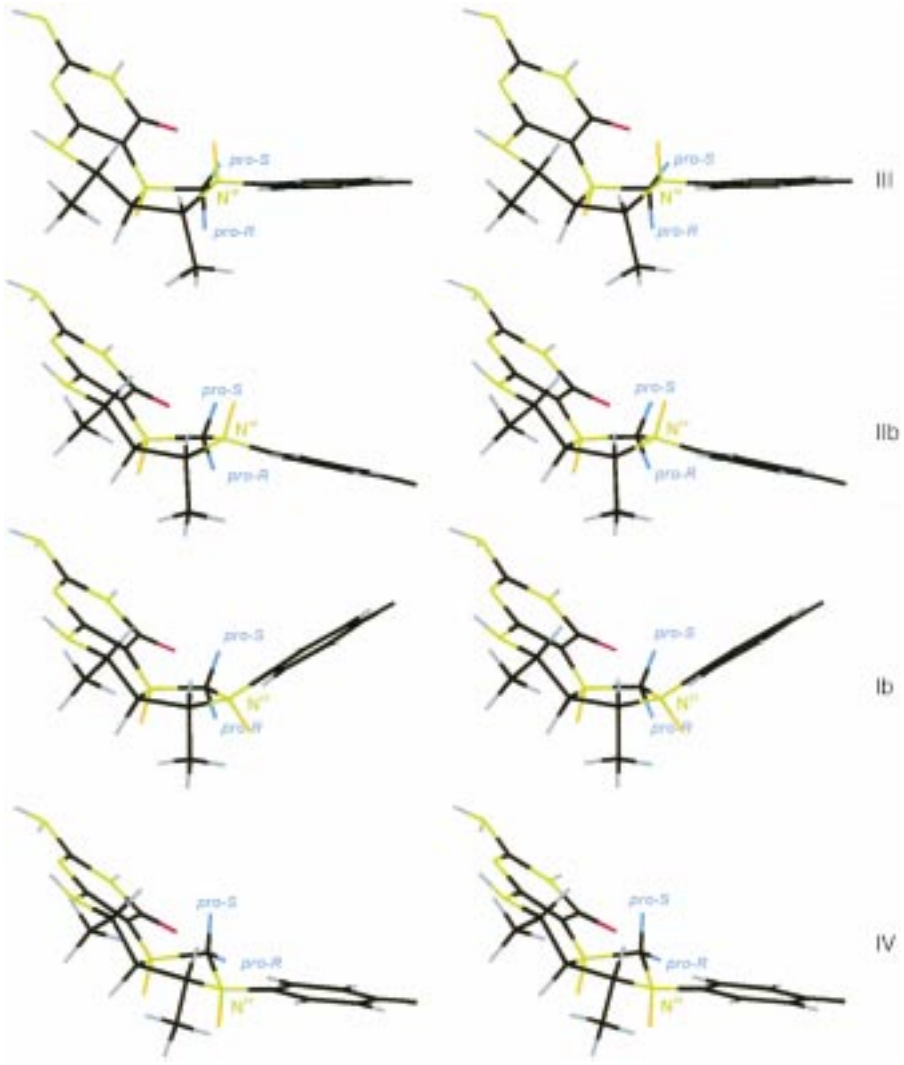

Figure 7. *Conformations (stereoview) of methylene-H_4MPT obtained by semiempirical AM1 calculations in vacuo.* ***Ib*** *is the conformation with the lowest energy and similar to the conformation free in solution as derived by NMR spectroscopy (Figure 6, conformation* ***Ia****). The imidazolidine ring is in an envelope conformation with the flap N^{10} below the ring and the* pro-S *hydrogen atom anticlinal to the lone electron pair at N^{10}. Conformation* ***IIb*** *is an alternative minimum with a heat of formation only $+2$ kJ mol^{-1} higher than that of conformation* ***Ib****. Conformation* ***IIb*** *is similar to the NMR-derived enzyme-bound conformation (Figure 6, conformation* ***IIa****). The imidazolidine ring is in an envelope conformation with the flap N^{10} above the ring and the* pro-R *hydrogen atom anticlinal to the lone electron pair of N^{10}.* ***III*** *and* ***IV*** *are proposed conformations for the transitions states: In* ***III*** *the* pro-R *hydrogen atom of C^{14a} is antiperiplanar to the lone electron pair of N^{10} (****IIb*** *$\rightarrow$****III****; $\Delta E_{23} = +29$ kJ mol^{-1}) and therefore reactive; in* ***IV*** *the reactive* pro-S *hydrogen atom of C^{14a} is antiperiplanar to the lone electron pair of N^{10} (****Ib*** *$\rightarrow$****IV****; $\Delta E_{14} = +53$ kJ mol^{-1}). For relative orientations of the lone electron pairs of N^5 and N^{10} to the bond of the* pro-S *and* pro-R *hydrogen atoms see Table 2. Lone electron pairs are shown in yellow, hydrogens in blue, nitrogens in green, carbons in black and oxygens in red.*

In conformation **Ib** (Figure 7) that corresponds to methylene-H_4MPT free in solution, the methylene *pro-S* C—H bond has an absolute dihedral angle of 117° with the lone electron pair of N^{10} (Figure 8 A and Table 2). In order to activate the *pro-S* C—H bond this angle can be increased to 180° by forcing conformation **Ib** into conformation **IV**. This deformation requires a ΔE_{14} of $+53$ kJ mol^{-1} (Figure 8 A). Between conformation **Ib** and **IIb** there is an inversion barrier of 16 kJ mol^{-1} (see Experimental Section). Conformation **III** can only be reached from conformation **Ib** via conformation **IIb**.

We also performed geometry optimisations for methylene-H_4F and found the conformations to be almost identical to those calculated for methylene-H_4MPT. In addition, the energy profiles for the conversion of conformation **Ib** of methylene-H_4F to the corresponding conformations **IIb**, **III** and **IV** are almost identical to those shown in Figure 8 for methylene-H_4MPT: ΔE_{23} was calculated to be $+35$ kJ mol^{-1} and ΔE_{14} to be $+51$ kJ mol^{-1}.

Reversed stereospecificity of methenyl-H_4MPT$^+$ reduction with $NaBD_4$ to methylene-H_4MPT

The quantum mechanical results indicate that almost twice as much energy is required to convert conformation **Ib** into **IV** for maximal activation of the methylene *pro-S* C—H bond than to convert conformation **IIb** into **III** for maximal activation of the methylene *pro-R* C—H bond of methylene-H_4MPT and methylene-H_4F. This may explain why the enzymatic dehydrogenation of methylene-H_4MPT and of methylene-H_4F always proceeds *Re*-face-specific.[11] Based on the principle of microscopic reversibility the back reaction should have the same stereospecificity as the forward reaction, and indeed it was shown that the enzymatic reduction of methenyl-H_4MPT$^+$ to methylene-H_4MPT with H_2 also proceeds *Re*-face-specific.[11] These results cannot explain, however, why the reduction of methenyl-H_4MPT$^+$ or methenyl-H_4F$^+$ with $NaBD_4$ to the respective methylene compounds is *Si*-face specific, leading to the incorporation of the hydride in the *pro-S* position.[15] An alternative mechanism must therefore be considered for the chemical reduction.

In the chemical reduction methenyl-H_4MPT$^+$ and methenyl-H_4F$^+$ react irreversibly with the negatively charged BD_4^- ion, whereas in the enzyme-catalysed reaction they react reversibly with neutral H_2, $F_{420}H_2$ or NAD(P)H. The energy-minimised conformations of methenyl-H_4MPT$^+$ indicate that the *Re*-face is sterically and electrostatically shielded by the oxygen atom at C^{4a} (Figure 9). Therefore, the approach of BD_4^- to the *Re*-face of the imidazoline ring can be expected to require more activation energy than the approach to the *Si*-face. Indeed, calculation of the minimum energy paths of AlH_4^- to methenyl-H_4MPT$^+$ reveals that the *Si*-face approach has a lower energy barrier than the *Re*-face

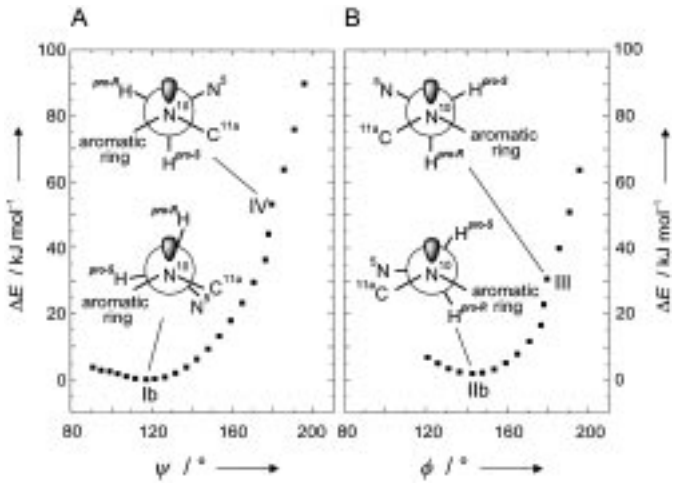

Figure 8. *Energy profile for the interconversion A) of conformation **Ib** of methylene-H_4MPT to conformation **IV** and B) of conformation **IIb** to conformation **III** in Figure 7. The difference of the heats of formation ΔE is plotted versus the absolute values of the dihedral angle (ψ or ϕ) between the lone electron pair of N^{10} and A) the C^{14a}—$H^{pro\text{-}S}$ bond and B) the C^{14a}—$H^{pro\text{-}R}$ bond. All energies are given relative to the energy of conformation **Ib**. The profiles are obtained from semiempirical quantum mechanical calculations by constraining the dihedral angle between the lone electron pair of N^{10} and the C^{14a}—$H^{pro\text{-}R}$ bond or the C^{14a}—$H^{pro\text{-}S}$ bond at specific values and by energy-minimising the remaining degrees of freedom using the molecular modeling package INSIGHT.[67] Conversion of conformation **Ib** into **IIb** involves the inversion at N^{10} with an estimated activation barrier of about +16 kJ mol^{-1} (see Experimental Section). Newman projections to illustrate the dihedral angle in conformations **I**–**IV** are shown for clarity.*

Table 2. *Dihedral angles between the lone electron pair of N^5 or N^{10} and the C^{14a}—$H^{pro\text{-}S}$ or C^{14a}—$H^{pro\text{-}R}$ bond for the conformations of methylene-H_4MPT shown in Figures 6 and 7.*

Conformation	Dihedral angle [°]			
	$N^5/H^{pro\text{-}S}$	$N^5/H^{pro\text{-}R}$	$N^{10}/H^{pro\text{-}S}$	$N^{10}/H^{pro\text{-}R}$
Ia	144	24	−137	−18
IIa	130	9	30	151
Ib	125	7	−117	2
IIb	121	2	23	143
III	95	−27	50	180
IV	172	48	−180	−48

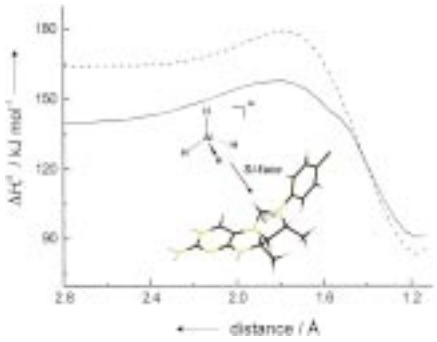

Figure 10. *Energy profiles for the reduction of methenyl-H_4MPT$^+$ with AlH_4^- approaching from either the* Si*-face (——) or the* Re*-face (- - - -) of the imidazolidine ring. The profiles show the lowest heat of formation of the two reactants for each distance as computed by using a semiempirical AM1 Hamiltonian. Distances are given in Å between the closest hydrogen atom of AlH_4^- and C^{14a}. Computation of the backward reaction (data not shown) reveals essentially an identical energy profile. Since corresponding semiempirical AM1 parameters for boron are not available, BD_4^- was modelled by AlH_4^-, which can also be regarded as a suitable hydride donor within this computational model system. The* Si*-face attack has the lower activation energy.*

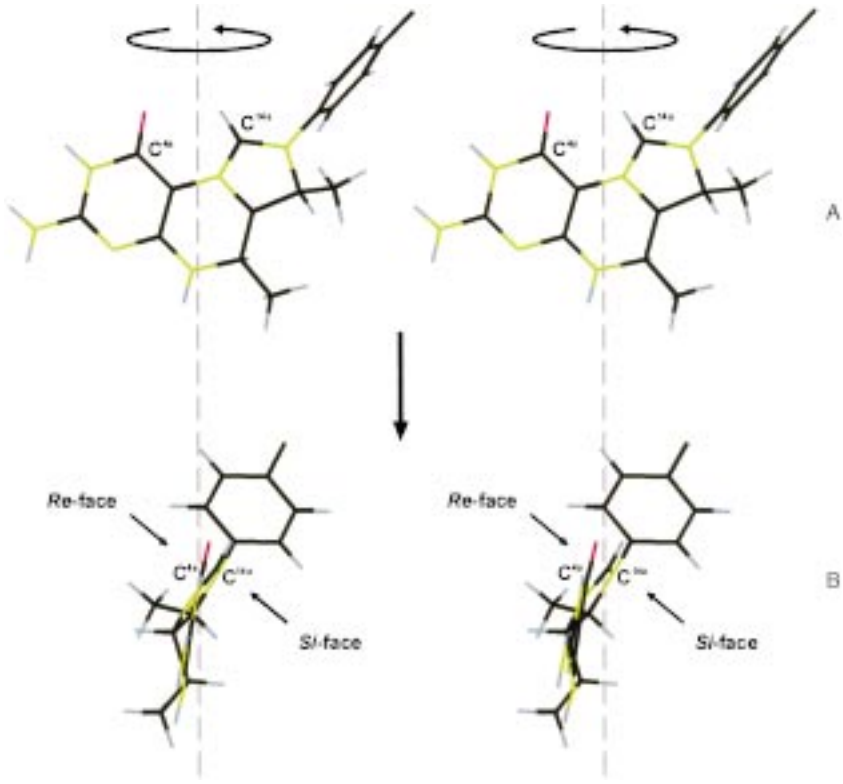

Figure 9. *Stereoview A) of the* Si*-face of methenyl-H_4MPT$^+$ and B) after rotation by 90° highlighting the shielding effect of the oxygen atom at C^{4a} on the accessibility of the positively charged C^{14a} to BD_4^-. Hydrogens are shown in blue, nitrogens in green, carbons in black and oxygen in red.*

approach (ca. 25 kJ mol^{-1}; (Figure 10). The same difference is obtained when calculating minimum energy paths for the reduction of methenyl-H_4F^+ with AlH_4^- (data not shown). AlH_4^- instead of BD_4^- was used in the calculations since parametrisation of the AlH_4^- anion was available and because AlH_4^- has been shown to react similarly to BD_4^-.[31]

The calculation of the minimum energy paths for the approach of AlH_4^- is not valid in a quantitative sense because the computation was performed in vacuo and because AlH_4^- is already in contact with the hydrophobic rings of methenyl-H_4MPT$^+$ while being pulled towards C^{14a}. Unfortunately, the errors of current solvation models are too high (ca. 14.6 kJ mol^{-1} for AMSOL)[32] to use them for extending the minimum energy paths to longer distances. Nevertheless, at van der Waals contact distances to C^{14a}, the calculations become more and more quantitatively correct and the results of the calculations with

AlH_4^- agree with the experimental finding that the reduction of methenyl-H_4MPT$^+$ and of methenyl-H_4F$^+$ with $NaBD_4$ proceeds with *Si*-face stereospecificity.[15]

Discussion

The enzyme-catalysed dehydrogenation of methylene-H_4MPT requires an activation energy of approximately $+50\,kJ\,mol^{-1}$ as determined for Hmd from *Methanothermobacter marburgensis* and from *Methanopyrus kandleri* from the temperature dependence of the activity.[30, 66] This indicates that the conformational change of methylene-H_4MPT upon enzyme binding associated with the generation of the transition state should not require more than $+50\,kJ\,mol^{-1}$. Semiempirical quantum mechanical calculations of the heats of formation (ΔH_f°) for the conformations **A** and **B** (Figure 2) revealed, however, that the required energy ΔE_{AB} associated with the conformational change **A** → **B** exceeds $+200\,kJ\,mol^{-1}$ both for methylene-H_4MPT and methylene-H_4F (see Results). The calculations indicate that conformational changes at N^5 are thermodynamically very unfavourable and that only conformational changes at N^{10} are possible. The calculations suggest a thermodynamically more favourable conformation for the transition state in which the *pro-R* C–H bond is in an antiperiplanar position only to the lone electron pair of N^{10}. In order to reach this transition state (conformation **III**, Figure 7) from the ground state (conformation **II b**, Figure 7), only $+29\,kJ\,mol^{-1}$ are required in case of methylene-H_4MPT and $+35\,kJ\,mol^{-1}$ in case of methylene-H_4F.

The newly proposed transition state raises the question whether one lone electron pair antiperiplanar to the *pro-R* C–H bond is sufficient to allow for the heterolytic cleavage of this C–H bond. It has previously been noted that the reactivity of a C–H bond correlates with the wave number of the C–H stretching band in the IR spectrum. C–H bonds with a very high reactivity have a relatively low wavenumber and vice versa. C–H bonds antiperiplanar to lone electron pairs of neighbouring nitrogen atoms generally show bands with wavenumbers below $2800\,cm^{-1}$ that are referred to as Bohlmann bands.[33–35] These bands are found for compounds such as perhydro-3a,6a,9a-triazaphenalene with a methine C–H bond in antiperiplanar position to three lone electron pairs of three neighbouring nitrogen atoms,[19–21] but also for compounds such as hexahydrojulolidine[36] and quinolizidine[37–40] with a methine C–H bond in an antiperiplanar position to only one lone electron pair (Figure 11). The presence of a Bohlmann band in hexahydrojulolidine and quinolizidine suggests that one perfectly antiperiplanar oriented lone electron pair should sufficiently activate the *pro-R* C–H bond.

The mechanism proposed for methylene-H_4MPT and methylene-H_4F dehydrogenation assumes that the four enzyme-catalysed reactions [Eqs. (1) – (4)] can in principle proceed only via two putative transition states, in which either the *pro-R* or the *pro-S* C–H bond of the substrate methylene group is maximally activated. The conformations of the two transition states, one of which is by $+24\,kJ\,mol^{-1}$ (methylene-H_4MPT) or $+16\,kJ\,mol^{-1}$ (methylene-H_4F) (difference of calculated heats of formation) more favoured than the other, differ significantly from the

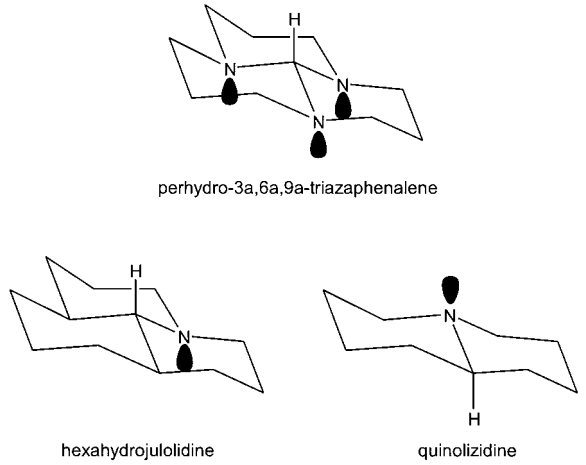

Figure 11. *Structures of perhydro-3a,6a,9a-triazaphenalene, of hexahydrojulolidine and of quinolizidine. The three compounds show Bohlmann bands[33–35] in their infrared spectra at 2450 cm^{-1},[19, 20] approximately 2750 cm^{-1}[36] and approximately 2750 cm^{-1},[38–40] respectively. Such wavenumbers are indicative of a reactive C–H bond.[15] For the crystal structure of perhydro-3a,6a,9a-triazaphenalene see ref. [63].*

substrate conformation in solution. Although with an estimated upper error of $10\,kJ\,mol^{-1}$ for the activation barrier, semiempirical quantum mechanical calculations are not very accurate, the energy differences of $+24\,kJ\,mol^{-1}$ and $+16\,kJ\,mol^{-1}$ seem nevertheless significant enough to explain the *Re*-face specificity of the dehydrogenation of methylene-H_4MPT and methylene-H_4F.

The NMR spectroscopical data revealed that upon binding of methylene-H_4MPT to Hmd the conformation of methylene-H_4MPT changes from **I a**, with the *pro-R* hydrogen atom synclinal, to **II a**, with the *pro-R* hydrogen atom anticlinal to the lone electron pair of N^{10} (Figure 6). Typically, binding of a ligand to its enzyme provides up to 10 – 15 $kJ\,mol^{-1}$ of energy,[41, 42] which is close in magnitude to the inversion barrier of $16\,kJ\,mol^{-1}$ between conformations **I b** and **II b** (see Experimental Section). A further increase in the dihedral angle between the lone electron pair of N^{10} and the C^{14a}–$H^{pro\text{-}R}$ bond by 29°, in order to reach the proposed transition state (conformation **III**, Figure 7), requires an energy ΔE_{23} of $+29\,kJ\,mol^{-1}$. It is the function of enzymes to funnel, by entropic guidance,[43] the populations of conformers to the transition state.[43, 44] Consistenly, the observed conformational change upon enzyme binding is the first step towards a low-energy transition state.

The mechanism proposed for enzymatic methylene-H_4MPT and methylene-H_4F dehydrogenation is similar in some respects to that proposed by Benner et al. for the enzymatic dehydrogenation of NAD(P)H.[45–47] In the active site, NAD(P)H was proposed to exist in either an *anti*-antiperiplanar conformation, with the *pro-R* C–H bond at C^4 activated, or in a *syn*-antiperiplanar conformation, with the *pro-S* C–H bond at C^4 activated.[43, 48, 49] The difference in potential energy between the two conformations was calculated to be approximately $+8\,kJ\,mol^{-1}$,[48] a difference much smaller than the difference of $+24\,kJ\,mol^{-1}$ or $+16\,kJ\,mol^{-1}$ we calculated for the two conformations of methylene-H_4MPT and methylene-H_4F, with either the *pro-R*

C–H bond or the *pro-S* C–H bond at C^{14a} maximally activated. The much smaller energy difference may be the reason why both *Re*-face stereospecific and *Si*-face stereospecific NAD(P)-dependent dehydrogenases are found.

Conclusions

By combining structural data from NMR spectroscopic measurements and theoretical predictions of activation energies from quantum chemical computations, a mechanism is proposed to explain the *Re*-face stereospecificity of the enzyme-catalysed dehydrogenation of methylene-H_4MPT and of methylene-H_4F. This mechanism is based on the theoretical prediction that only half the energy is required to force the *pro-R* hydrogen atom into an activated antiperiplanar conformation relative to the lone electron pair of N^{10} than to force the *pro-S* hydrogen atom into the antiperiplanar conformation. Confidence in the theoretical calculations is provided by the fact that a) the two computed minimum energy conformations are in good agreement with the NMR-based structures of methylene-H_4MPT in solution and when enzyme-bound and the fact that b) the computed energy profiles for the reduction of methenyl-H_4MPT^+ with AlH_4^- correctly predict the observed *Si*-face-specific hydrogenation of methenyl-H_4MPT^+ and methenyl-H_4F^+ in solution by $NaBD_4$.

Experimental Section

Enzyme and coenzyme preparation: Hmd was purified from *Methanothermobacter marburgensis*[50] (formerly *Methanobacterium thermoautotrophicum*).[28] The purified enzyme with a molecular mass of 37831 Da exhibited a specific activity of 1200 U mg^{-1} at 65 °C and of approximately 10 U mg^{-1} at 0 °C as determined photometrically by following the dehydrogenation of methylene-H_4MPT at pH 6.0 and 336 nm.[50] Methylene-H_4MPT and methenyl-H_4MPT^+ were prepared as described by Breitung et al.[51] Since Hmd is inactivated in the presence of O_2 and methylene-H_4MPT is susceptible to autoxidation, all experiments were performed under strictly anaerobic conditions (where possible) in an anaerobic glove box (Coy Laboratory Products Inc.) filled with 95% N_2/5% H_2 and containing palladium catalyst for the continuous removal of O_2.

NMR spectroscopy: NMR spectra were recorded at 0 °C on a Bruker DRX 600 MHz NMR spectrometer. The NMR tubes contained 0.5 mL of a solution of 50 mM potassium phosphate (pH 7.8) in H_2O/D_2O (9:1), 1 mM methylene-H_4MPT and, when indicated, 0.3 mM Hmd (6.0 mg/0.5 mL). The gas phase above the solution consisted of 100% H_2.

2D NOESY spectra in H_2O/D_2O (9:1) were collected by using standard NOESY pulse sequences with 1024 or 2048 complex points in t_2 over a spectral width of 6024.1 Hz. The mixing time τ_m was varied between 15 and 200 ms. For each spectrum 512 t_1 experiments with 32 scans were acquired with a recycle delay of 3 s. Water suppression was either achieved by a WATERGATE pulse scheme[52] or a low-power presaturation pulse during recycling delay and mixing time.[53] Spectra were zero-filled to 2048 points in ω_1 and 1024 points in ω_2. A 90°-shifted squared sinebell window function was applied for apodisation prior to Fourier transformation in both dimensions. Automated baseline correction was applied in both dimensions. For 1D spectra an exponential window function with 0.5 Hz line broadening was applied and all spectra were referenced to the H_2O signal at $\delta = 5.01$ at 0 °C.

NMR data were processed using the software programs FELIX 98 (MSI, Inc., San Diego, CA) and XWINNMR 2.6 (Bruker Instruments, Rheinstetten). Resonance peaks were assigned based on published spectra.[11] Nuclear Overhauser effect (NOE) cross-peak integrals were integrated using the program FELIX. Cross-relaxation rates were determined from the initial slope of a polynomial fit of the cross-peak integrals as a function of the mixing time. We took the $H^{2b/6b}/H^{3b/5b}$ cross-relaxation rate as reference since this distance does not change upon binding to the enzyme ($r_{ref} = 2.46$ Å). Also the cross relaxation rate of this peak is not affected by a rotational mobility of the aromatic ring. For methylene-H_4MPT free in solution, NOE distance restraints were derived directly from the cross-relaxation rates.

In the presence of Hmd the measured NOE cross-peaks are the sum of contributions from the enzyme-bound and the free conformations of methylene-H_4MPT. To obtain distance restraints for the enzyme-bound conformation we subtracted the contributions of the free conformation according to the following procedure: The $H^{2b/6b}/H^{3b/5b}$ cross-relaxation rates in the absence of enzyme (σ^a_{ref}) and in the presence of enzyme (σ^p_{ref}) were determined from the initial slope of a polynomial fit of the $H^{2b/6b}/H^{3b/5b}$ cross-peak integral as a function of the mixing time, divided by the sum over the well-dispersed diagonal peak of $H^{2b/6b}$ and the integrals I^a_{ref} and I^p_{ref}, respectively, over all cross-peaks with the resonance of $H^{2b/6b}$ in ω_2. These absolute rates $\sigma^a_{ref} = 0.2$ Hz and $\sigma^p_{ref} = 1.5$ Hz and the molecular masses M of Hmd (37831 Da) and methylene-H_4MPT (775 Da) were used to determine the population p^b of the bound form of methylene-H_4MPT according to Equation (5);

$$\frac{\sigma^p_{ref}}{\sigma^a_{ref}} = \frac{p^b M_{Hmd} + (1-p^b) M_{methylene\text{-}H_4MPT}}{M_{methylene\text{-}H_4MPT}} \quad (5)$$

taking into account that the correlation time is linear with the molecular mass. The percentage of methylene-H_4MPT bound to the enzyme is $p^b \times 100$. The correlation time for the free form is 840 ps as determined from σ^a_{ref} and the distance between $H^{2b/6b}$ and $H^{3b/5b}$. At 600 MHz, $J(2\omega_H)$ is already negligable since it contributes less than 10% to the spectral density.

The integrals I^a_{ref} and I^p_{ref} for all spectra served to calibrate all cross-peak integrals to unity. The integrals I^a without or I^p with enzyme, respectively, of the A,B cross-peak reporting the A,B distance were scaled for each mixing time with the integrals I^a_{ref} and I^p_{ref}, respectively. σ^a_{A-B} and σ^p_{A-B} were obtained from the initial slope to the polynomial fit of I^a/I^a_{ref} and I^p/I^p_{ref}, respectively (Table 1). The distances of the bound form were determined according to Equation (6):

$$\frac{r_{A-B(bound)}}{r_{ref}} = \sqrt[6]{\frac{\sigma^p_{ref} - (1-p^b)\,\sigma^a_{ref}}{\sigma^p_{A-B} - (1-p^b)\,\sigma^a_{A-B}}} \quad (6)$$

Calculation of the conformation of methylene-H_4MPT from NMR data: To obtain an energetically favourable structure that was consistent with the NMR data, we generated a computer model of methylene-H_4MPT. A simulated annealing and energy minimisation protocol was then carried out using the program X-PLOR[54] with a force field derived from the two three-dimensional structures of methylene-H_4F bound to crystallised thymidylate synthase[55] by using the LEARN command in X-PLOR.[56] This command derives ideal values for covalent interactions from averages over a set of coordinates, and force constants from their variance, analogous to the procedure used to derive the energy parameters commonly used in X-ray crystallographic refinement.[57] The calculations were carried out in vacuo without electrostatic terms. Nonbonded parameters were taken from the CHARMm PARAM 19 force field.[58] The

simulated annealing protocol consisted of 120 000 steps with a time step of 0.2 fs of molecular dynamics starting at a temperature of 2000 K and slowly cooling to 100 K. This was followed by 200 steps of conjugate gradient minimisation. Other minimised parameters were set as described by Nilges and O'Donoghue.[54] The interproton distances determined from the transferred NOE experiments were used as restraints allowing a 10% uncertainty in distances without energy penalty. The energy-minimised model was then carefully checked to ensure that it obeyed the NMR distance restraints. In the conformational search procedure, N^{10} was allowed to be flexible, whereas all the other carbon and nitrogen atoms in the pterin moiety including N^5 were restrained during the calculation to the amount of planarity found in the crystal structure of methylene-H_4F bound to thymidylate synthase.[55] The search was repeated with two different starting geometries derived from this crystal structure. All the individual conformations found were then evaluated by comparison of internuclear distances with the experimentally determined distance restraints to find the conformation which best agreed with the NMR data. When none of the structures fully satisfied the NMR distance restraints, ensembles of structures were generated by stepwise rotating the aromatic ring and the methyl groups. NOE cross-relaxation rates were calculated for these structures and combined into an effective cross-relaxation rate of the ensemble according to the following procedure:

Rotations about the dihedral angles about the N^{10}—C^{1b} bond for the aromatic ring and about the C^{7a}—C^{13a} and C^{11a}—C^{12a} bonds for the methyl groups were performed with the program Insight II (MSI, Inc.) in steps of 5°. Distances of fixed protons H^f to the aromatic protons H^a were treated with the r^{-6} sum assuming dynamics that are slow compared to the correlation time [Eq. (7)],[59]

$$\sigma_{af} = \frac{1}{2\pi}\int_0^{2\pi} \frac{d\varphi}{|(\mathbf{H^a} - \mathbf{H^f})|^6} \quad (7)$$

with φ being the dihedral angle of the aromatic ring and $\mathbf{H^a}$ and $\mathbf{H^f}$ being the vectors to the nuclei of H^a and H^f, respectively. As mentioned before, the integration [0, 2π] was replaced by the sum [0°, 5°, ..., 360°] and was evaluated by a FORTRAN program.

Distances between fixed protons H^f to the methyl protons H^m were calculated by using Equation (8) (where φ_1 and φ_2 are both dihedral angles about the Me—C bonds) assuming dynamics that are fast compared to the correlation time.

$$\sigma_{mf} = \frac{1}{(2\pi)^2}\int_0^{2\pi}\int_0^{2\pi} \frac{0.5\left(3\frac{\left((\mathbf{H^m}\text{-}\mathbf{H^f})(\varphi_1)\ (\mathbf{H^m}\text{-}\mathbf{H^f})(\varphi_2)\right)^2}{\left|(\mathbf{H^m}\text{-}\mathbf{H^f})(\varphi_1)\right|^2\left|(\mathbf{H^m}\text{-}\mathbf{H^f})(\varphi_2)\right|^2} - 1\right)}{\left|(\mathbf{H^m}\text{-}\mathbf{H^f})(\varphi_1)\right|^3\left|(\mathbf{H^m}\text{-}\mathbf{H^f})(\varphi_2)\right|^3} d\varphi_1 d\varphi_2 \quad (8)$$

Distances between protons of the aromatic ring to protons of the methyl groups were calculated by rotating each in steps of 5° using Equation (9) assuming a fast rotation of the methyl groups relative to the aromatic ring:[54] φ_1 and φ_3 are independently varied angles about the Me—C bond and φ_2 and φ_4 about the C—phenyl bond.

$$\sigma_{am} = \frac{1}{(2\pi)^4}\int_0^{2\pi}\int_0^{2\pi}\int_0^{2\pi}\int_0^{2\pi} \frac{0.5\left(3\frac{\left((\mathbf{H^a}\text{-}\mathbf{H^m})(\varphi_1,\varphi_2)\ (\mathbf{H^a}\text{-}\mathbf{H^m})(\varphi_3,\varphi_4)\right)^2}{\left|(\mathbf{H^a}\text{-}\mathbf{H^m})(\varphi_1,\varphi_2)\right|^2\left|(\mathbf{H^a}\text{-}\mathbf{H^m})(\varphi_3,\varphi_4)\right|^2} - 1\right)}{\left|(\mathbf{H^a}\text{-}\mathbf{H^m})(\varphi_1,\varphi_2)\right|^3\left|(\mathbf{H^a}\text{-}\mathbf{H^m})(\varphi_3,\varphi_4)\right|^3} d\varphi_1 d\varphi_2 d\varphi_3 d\varphi_4 \quad (9)$$

From the averaged rates the theoretical distances were calculated by referencing to the reference rate and the reference distance according to Equation (10).

$$\bar{r}_{A\text{-}B} = r_{ref}\sqrt[6]{\frac{\sigma_{ref}}{\bar{\sigma}_{ref}}} \quad (10)$$

The internuclear distances of the ensemble of structures fulfil the experimental NOE cross-relaxation rates to within 10%. The structures shown in Figure 6 represent the ensemble best fitting minimum.

Semiempirical quantum mechanical calculations of the conformations of methylene-H_4MPT, methylene-H_4F, methenyl-H_4MPT$^+$ and methenyl-H_4F$^+$: The quantum chemical calculations were carried out using the program package VAMP (G. Rauhut, A. Alex, J. Chandrasekhar, T. Steinke, W. Sauer, B. Beck, M. Hutter, P. Gedeck, T. Clark, VAMP Version 6.5, Oxford Molecular, Erlangen, **1997**). The AM1 Hamiltonian[29] was applied to obtain all results and the Eigenvector Following[60] algorithm was used throughout all calculations to optimise each molecular system to a gradient norm below $+1.7$ kJ mol^{-1} Å^{-1}. The molecular systems considered were derived from the structures of N^5,N^{10}-methylene-H_4MPT or N^5,N^{10}-methylene-H_4F (Figure 1). R was CH_2-CH_2-OH in the case of methylene-H_4MPT and CONH-CH_3 in the case of methylene-H_4F. The computation of the energy profile given in Figure 8 was carried out by individual energy minimisations of the structure of methylene-H_4MPT with the dihedral angle between the lone electron pair orbital of N^{10} and the C^{14a}—$H^{pro\text{-}R}$ bond constrained to defined values. For the reaction profiles given in Figure 10 steps of 0.05 Å were chosen. Since corresponding semiempirical AM1 parameters for boron are not available, BD_4^- was modelled by AlH_4^-, which can also be regarded as a suitable hydride donor within this computational model system.

To computationally estimate an upper limit of the inversion barrier at N^{10}, the dihedral angle C^{1b}-N^{10}-C^{11a}-C^{6a} (Figure 1) was altered from $+126°$ to $+249°$ in steps of 5°. The highest point on this reaction path had a dihedral angle of 166° and is 16 kJ mol^{-1} higher in energy than conformer **Ib** (Figure 7).

All NMR measurements were conducted at the European Large Scale Facility for Biomolecular NMR (ERBCT95-0034) at the University of Frankfurt. This work was supported by the Max-Planck-Gesellschaft, by the Deutsche Forschungsgemeinschaft and by the Fonds der Chemischen Industrie. S.B. is supported by a Kekulé stipend of the Fonds der Chemischen Industrie and is a member of the Graduiertenkolleg "Chemische und biologische Synthese von Wirkstoffen" at the University of Frankfurt.

[1] R. K. Thauer, *Microbiology* **1998**, *144*, 2377 – 2406.
[2] B. E. H. Maden, *Biochem. J.* **2000**, *350*, 609 – 629.
[3] L. Chistoserdova, J. A. Vorholt, R. K. Thauer, M. E. Lidstrom, *Science* **1998**, *281*, 99 – 102.
[4] J. A. Vorholt, L. Chistoserdova, S. M. Stolyar, R. K. Thauer, M. E. Lidstrom, *J. Bacteriol.* **1999**, *181*, 5750 – 5757.
[5] J. A. Vorholt, L. Chistoserdova, M. E. Lidstrom, R. K. Thauer, *J. Bacteriol.* **1998**, *180*, 5351 – 5356.
[6] R. K. Thauer, A. R. Klein, G. C. Hartmann, *Chem. Rev.* **1996**, *96*, 3031 – 3042.
[7] G. Buurman, S. Shima, R. K. Thauer, *FEBS Lett.* **2000**, *485*, 200 – 204.
[8] C. H. Hagemeier, L. Chistoserdova, M. E. Lidstrom, R. K. Thauer, J. A. Vorholt, *Eur. J. Biochem.* **2000**, *267*, 3762 – 3769.
[9] M. Allaire, Y. G. Li, R. E. MacKenzie, M. Cygler, *Structure* **1998**, *6*, 173 – 182.
[10] L. J. Slieker, S. J. Benkovic, *J. Am. Chem. Soc.* **1984**, *106*, 1833 – 1838.
[11] J. Schleucher, C. Griesinger, B. Schwörer, R. K. Thauer, *Biochemistry* **1994**, *33*, 3986 – 3993.
[12] A. R. Klein, R. K. Thauer, *Eur. J. Biochem.* **1995**, *227*, 169 – 174.
[13] C. H. Hagemeier, S. Bartoschek, C. Griesinger, R. K. Thauer, J. A. Vorholt, *FEBS Lett.* **2001**, *494*, 95 – 98.
[14] A. Berkessel, R. K. Thauer, *Angew. Chem.* **1995**, *107*, 2418 – 2421; *Angew. Chem. Int. Ed. Engl.* **1995**, *34*, 2247 – 2250.

[15] B. H. Geierstanger, T. Prasch, C. Griesinger, G. Hartmann, G. Buurman, R. K. Thauer, *Angew. Chem.* **1998**, *110*, 3491 – 3494; *Angew. Chem. Int. Ed.* **1998**, *37*, 3300 – 3303.
[16] J. Cioslowski, G. Boche, *Angew. Chem.* **1997**, *109*, 165 – 167; *Angew. Chem. Int. Ed. Engl.* **1997**, *36*, 107 – 109.
[17] A. P. Scott, B. T. Golding, L. Radom, *New J. Chem.* **1998**, *22*, 1171 – 1173.
[18] J. H. Teles, S. Brode, A. Berkessel, *J. Am. Chem. Soc.* **1998**, *120*, 1345 – 1346.
[19] J. M. Erhardt, J. D. Wuest, *J. Am. Chem. Soc.* **1980**, *102*, 6363 – 6364.
[20] J. M. Erhardt, E. R. Grover, J. D. Wuest, *J. Am. Chem. Soc.* **1980**, *102*, 6365 – 6369.
[21] T. J. Atkins, *J. Am. Chem. Soc.* **1980**, *102*, 6364 – 6365.
[22] J. C. Fontecilla-Camps, C. E. Bugg, C. Temple, Jr., J. D. Rose, J. A. Montgomery, R. L. Kisluik, *J. Am. Chem. Soc.* **1979**, *101*, 6114 – 6115.
[23] M. Poe, L. M. Jackman, S. J. Benkovic, *Biochemistry* **1979**, *18*, 5527 – 5530.
[24] R. Kalbermatten, W. Städeli, J. H. Bieri, M. Viscontini, *Helv. Chim. Acta* **1981**, *64*, 2627 – 2635.
[25] J. P. Albrand, B. Birdsall, J. Feeney, G. C. K. Roberts, A. S. V. Burgen, *Int. J. Biol. Macromol.* **1979**, *1*, 37 – 41.
[26] G. M. Clore, A. M. Gronenborn, *J. Magn. Reson.* **1982**, *53*, 423 – 442.
[27] B. D. Sykes, *Curr. Opin. Biotechnol.* **1993**, *4*, 392 – 396.
[28] A. Wasserfallen, J. Nolling, P. Pfister, J. Reeve, E. C. de Macario, *Int. J. Syst. Evol. Microbiol.* **2000**, *50*, 43 – 53.
[29] M. J. S. Dewar, E. G. Zoebisch, E. F. Healy, J. J. P. Stewart, *J. Am. Chem. Soc.* **1985**, *107*, 3902 – 3909.
[30] K. Ma, C. Zirngibl, D. Linder, K. O. Stetter, R. K. Thauer, *Arch. Microbiol.* **1991**, *156*, 43 – 48.
[31] J. March, *Advanced Organic Chemistry*, 4th ed., Wiley, New York, **1992**.
[32] G. D. Hawkins, C. J. Cramer, D. G. Truhlar, *J. Phys. Chem. B* **1998**, *102*, 3257 – 3271.
[33] F. Bohlmann, *Angew. Chem.* **1957**, *20*, 641 – 642.
[34] P. J. Krueger, J. Jan, *Can. J. Chem.* **1970**, *48*, 3236 – 3248.
[35] R. Jeyaraman, T. Ravindran, M. Sujatha, M. Venkatraj, *Indian J. Chem. Sect. B* **1999**, *38*, 52 – 55.
[36] F. Bohlmann, C. Arndt, *Chem. Ber.* **1958**, *91*, 2167 – 2175.
[37] F. Bohlmann, *Chem. Ber.* **1958**, *91*, 2157 – 2167.
[38] C. D. Johnson, R. A. Y. Jones, A. R. Katritzky, C. R. Palmer, K. Schofield, R. J. Wells, *J. Chem. Soc. Chem. Commun.* **1965**, 6797 – 6806.
[39] G. W. Gribble, R. B. Nelson, *J. Org. Chem.* **1973**, *38*, 2831 – 2834.
[40] F. W. Vierhapper, E. L. Eliel, *J. Org. Chem.* **1979**, *44*, 1081 – 1087.
[41] J. Boström, P.-O. Norrby, T. Liljefors, *J. Comput. Aided Mol. Des.* **1998**, *12*, 383 – 396.
[42] M. C. Nicklaus, S. Wang, J. S. Driscoll, G. W. Milne, *Bioorg. Med. Chem.* **1995**, *3*, 411 – 428.
[43] L. Young, C. B. Post, *Biochemistry* **1996**, *35*, 15 129 – 15 133.
[44] R. Castillo, J. Andrés, V. Moliner, *J. Am. Chem. Soc.* **1999**, *121*, 12 140 – 12 147.
[45] S. A. Benner, *Experientia* **1982**, *38*, 633 – 637.
[46] K. P. Nambiar, D. M. Stauffer, P. A. Kolodziej, S. A. Benner, *J. Am. Chem. Soc.* **1983**, *105*, 5886 – 5890.
[47] S. A. Benner, K. P. Nambiar, G. K. Chambers, *J. Am. Chem. Soc.* **1985**, *107*, 5513 – 5517.
[48] Ö. Almarsson, T. C. Bruice, *J. Am. Chem. Soc.* **1993**, *115*, 2125 – 2138.
[49] D. J. Creighton, N. S. R. K. Murthy in *The Enzymes*, *Vol. XIX* (Eds.: D. S. Sigman, P. D. Boyer), 3rd ed., Academic Press, San Diego, **1990**, pp. 323 – 421.
[50] C. Zirngibl, R. Hedderich, R. K. Thauer, *FEBS Lett.* **1990**, *261*, 112 – 116.
[51] J. Breitung, G. Börner, S. Scholz, D. Linder, K. O. Stetter, R. K. Thauer, *Eur. J. Biochem.* **1992**, *210*, 971 – 981.
[52] M. Piotto, V. Saudek, V. Sklenát, *J. Biomol. NMR* **1992**, *2*, 661 – 665.
[53] B. H. Meier, R. R. Ernst, *J. Am. Chem. Soc.* **1979**, *101*, 6441 – 6442.
[54] M. Nilges, S. I. O'Donoghue, *Prog. Nucl. Magn. Reson. Spectrosc.* **1998**, *32*, 107 – 139.
[55] C. R. Sage, M. D. Michelitsch, T. J. Stout, D. Biermann, R. Nissen, J. Finer-Moore, R. M. Stroud, *Biochemistry* **1998**, *37*, 13 893 – 13 901.
[56] A. Hodel, T. Simonson, R. O. Fox, A. T. Brünger, *J. Phys. Chem.* **1993**, *97*, 3409 – 3417.
[57] R. Engh, R. Huber, *Acta Crystallogr. Sect. A* **1991**, *47*, 392 – 400.
[58] B. R. Brooks, R. E. Bruccoleri, B. D. Olafson, D. J. States, S. Swaminathan, M. Karplus, *J. Comput. Chem.* **1983**, *4*, 187 – 217.
[59] C. M. Fletcher, D. N. M. Jones, R. Diamond, D. Neuhaus, *J. Biomol. NMR* **1996**, *8*, 292 – 310.
[60] J. Baker, *J. Comput. Chem.* **1986**, *7*, 385 – 395.
[61] P. van Beelen, A. P. M. Stassen, J. W. G. Bosch, G. D. Vogels, W. Guijt, C. A. G. Haasnoot, *Eur. J. Biochem.* **1984**, *138*, 563 – 571.
[62] M. Poe, S. J. Benkovic, *Biochemistry* **1980**, *19*, 4576 – 4582.
[63] R. L. Beddoes, W. D. Edwards, J. A. Joule, O. S. Mills, J. D. Street, *Tetrahedron Lett.* **1987**, *43*, 1903 – 1920.
[64] Abbreviations: H_4MPT = tetrahydromethanopterin, H_4F = tetrahydrofolate, methylene-H_4MPT = N^5,N^{10}-methylene-H_4MPT, methylene-H_4F = N^5,N^{10}-methylene-H_4F, methenyl-H_4MPT$^+$ = N^5,N^{10}-methenyl-H_4MPT$^+$, methenyl-H_4F$^+$ = N^5,N^{10}-methenyl-H_4F$^+$.
[65] M. C. Hutter, V. Helms, unpublished results.
[66] G. Buurman, R. K. Thauer, unpublished results.
[67] INSIGHT, version II, MSI, Inc., San Diego, CA.

Received: November 15, 2000 [F 157]